Analyst

PAPER

View Article Online
View Journal

Cite this: DOI: 10.1039/c7an01577a

Rapid and sensitive detection of neuron specific enolase with a polydopamine coated plasmonic chip utilizing a rear-side coupling method†

M. Toma, [a] S. Izumi[b] and K. Tawa *[a]

A rapid and sensitive detection of a cancer marker, neuron specific enolase (NSE), is demonstrated by using a disposable silver plasmonic chip functionalized with a mussel-inspired polydopamine (PDA) coating. A plasmonic chip consisting of a diffraction grating coated with a silver thin film is used for the excitation of propagating surface plasmon resonance through a rear-side grating coupling method. Simple and quick bio-functionalization of the sensor surface is performed by PDA coating which requires 20 min for deposition, and allows direct attachment of the capture antibody without using any coupling agents. A fluorescence based sandwich immunoassay is used for the detection of NSE by utilizing surface plasmon enhanced fluorescence (SPF) spectroscopy. The developed biosensor scheme provides approximately linear sensor responses for the sample containing NSE with the concentration around the clinically important value (12 ng mL^{-1}) in both buffer and diluted human serum (25 vol% to a buffer solution). The detection limit for NSE is 0.5 ng mL^{-1} (11 pM) and 1.4 ng mL^{-1} (30 pM) in a buffer solution and diluted human serum, respectively. The presented biosensor scheme requires a small amount of the sample down to 10 μL in human serum and a short incubation time (15 min) of the sample solution containing NSE, enabling less invasive and rapid detection of NSE. This is the first example of the sensitive sandwich immunoassay demonstrated by using a plasmonic chip for the measurement of the sample dissolved in a complex medium with a rear side coupling method, which progresses the universal use of the SPF biosensors with a disposable plasmonic chip.

Received 22nd September 2017,
Accepted 12th December 2017

DOI: 10.1039/c7an01577a

rsc.li/analyst

Introduction

Over the last years, the importance of molecular diagnosis has been increasing along with the development of biomarkers for the early diagnostics of serious diseases such as cancers.[1,2] In the case of cancer treatment, the serum levels of several biomarkers are examined and monitored for the diagnosis and the follow-up observation after therapy. Enzyme-linked immunosorbent assay (ELISA) is one of the established methods used for the detection of biomarkers in clinical samples. Though the amount of biomarkers can be sensitively and quantitatively detected by ELISA, the detection process consists of multiple steps and requires expertise to obtain reliable examination results. Optical biosensors utilizing fluorescence signals arise as an alternative method for the highly sensitive detection of target biomolecules. The surface plasmon enhanced fluorescence (SPF) biosensors have attracted great attention due to their excellent ability for the rapid and sensitive detection of the target analyte.[3,4] By using an enhanced electromagnetic field of SPs in the vicinity of metal sensor surfaces for the excitation of fluorophores, an advanced limit of detection down to a femtomolar level has been demonstrated for the detection of biomarkers including tumor markers.[5,6]

As the detection sensitivity and usability of an SPF biosensor are varied depending on the sensor surface architecture, plasmonic mode and the optical setup, an appropriate design has to be chosen to maximize the sensor performance depending on the purpose of use. The attenuated total reflection (ATR) method based on a prism coupler is conventionally used for the excitation of propagating surface plasmons. In addition to its extended electromagnetic (EM) field reaching up to hundreds of nanometers from the sensor surface, the prism coupling method is useful for the quantitative analysis of molecular binding events by combining the refractometric

[a]Department of Applied Chemistry for Environment, School of Science and Technology, Kwansei Gakuin University, Sanda, 669-1337, Japan. E-mail: ktawa@kwansei.ac.jp; Fax: +81-79-565-9729; Tel: +81-79-565-9758
[b]Department of Chemistry, Graduate School of Science and Technology, Kwansei Gakuin University, Sanda, 669-1337, Japan

†Electronic supplementary information (ESI) available: The schematic drawing of the optical setup; a plot of the fluorescence signals induced by the non-specific adsorption as a function of the dilution ratio of human serum. See DOI: 10.1039/c7an01577a

detection referred to as surface plasmon resonance spectroscopy. Nevertheless, the use of the prism coupling method is limited as it requires relatively bulky optical setup and a high refractive index prism. The grating coupling method (GC-SPR) was later introduced into SPF spectroscopy as a simpler method to exploit the EM field of propagating SPs with universal optical setups.[7] In the grating coupling method, a diffraction grating coated with a thin metal film is used to fulfill the resonance conditions, and the plasmonic properties can be tuned by the structure of the grating, namely the pitch and the modulation depth. In our laboratory, we have established novel SPF biosensors utilizing GC-SPR with a disposable substrate called a plasmonic chip.[6,8] As the fabrication of a plasmonic chip relies on the UV nanoimprint method followed by deposition of a metal film, the replication of the same grating structures is achieved. Though the localized surface plasmons (LSPs) excited on the metal nanostructures are also a powerful tool as LSPs can be induced by direct irradiation of light,[9,10] our plasmonic chips hold advantages of the extended EM field of propagating SPs with controllable plasmonic properties. Our previous study revealed that the detection sensitivity in terms of the detection limit of the target analyte can be improved up to three orders of magnitude by using a plasmonic chip with respect to a planar glass substrate.[11]

Herein, we developed a novel SPF biosensor for the detection of a tumor marker, neuron specific enolase (NSE), by using the polydopamine coated silver plasmonic chip as a perspective of the usage of the plasmonic chip in clinical diagnostics. Neuron specific enolase (NSE) also referred to as enolase 2 (ENO2) is known as one of the biomarkers of small cell lung cancer (SCLC).[1,12] As lung cancer causes a high mortality ratio with respect to the other cancers,[13] the early diagnostics using biomarkers in serum are highly required. The serum concentration of NSE of a healthy person is reported to be up to 12–13 ng mL^{-1}, and a cut-off value of 16–25 ng mL^{-1} has been proposed for the diagnosis of SCLC.[12,14,15] Polydopamine (PDA) coating was employed for quick and easy biofunctionalization of the plasmonic chip. PDA thin films are known as the mussel-inspired adhesive, which can coat various solid surfaces by simply applying the dopamine solution and incubating for several tens of minutes.[16,17] On the PDA coated surface, biomolecules can be directly anchored through the Quinone Schiff base reaction and/or Michael addition of amine or thiol groups included in the biomolecules.[18] We have reported the utility of PDA thin films as the linker layer of the capture antibody in SPF biosensors, and sensitive detection of the cytokine marker interleukin-6 was performed by utilizing the conventional prism coupling method.[19] In this study, we extended the usage of the PDA coating for the surface functionalization of the disposable plasmonic chip, and characterized the sensing performance for the detection of biomolecules in a complex medium namely human serum for the first time. For the excitation of GC-SPR, the advanced optical configuration referred to as the rear-side coupling method based on the back side illumination of the excitation laser beam was employed in order to suppress the background signals. The developed NSE biosensor based on the fluorescence sandwich immunoassay exhibited a linear sensor response for the NSE concentrations from 1 ng mL^{-1} to 100 ng mL^{-1}, which covers the clinically important concentration region. The obtained limit of detection of NSE was 0.5 ng mL^{-1} in buffer solution and 1.4 ng mL^{-1} (5.6 ng mL^{-1}) in diluted human serum (original serum concentration), with a short incubation time of NSE (15 min). By using the diluted sample, the sample volume necessary for the measurement is reduced to 10 μL enabling less invasive sampling. With respect to the conventional approach such as ELISA and recently reported studies based on the SPF method using LSPR,[10] our NSE biosensor can provide the comparable detection sensitivity achieved by using the shortened time of the assay procedure within 60 min including the immobilization process of the capture antibody.

Experimental

Materials

All the chemicals were used as received. Recombinant human neuron specific enolase (46 kDa), two kinds of purified anti-human NSE antibodies, and a reagent diluent (DY997) were purchased from R&D Systems. The used detection antibody (d-Ab) was biotinylated. The Cy5-labelled streptavidin (Cy5-SA) was obtained from GE Healthcare, and used for fluorescence detection. The concentration of d-Ab and Cy5-SA was adjusted to 2.5 μg mL^{-1} and 10 nM, respectively. 10 mM Tris buffer (pH = 8.5) was prepared by mixing 10 mM tris(hydroxymethyl) aminomethane solution and 10 mM tris(hydroxymethyl) aminomethane hydrochloride solution. The buffer salts of Tris buffer were purchased from Nacalai tesque. Phosphate buffered saline (PBS) was prepared with a PBS tablet and MilliQ water. PBS-tween (PBST) was prepared by adding 0.05 v% of Tween 20 into PBS buffer. The assay diluent was prepared by mixing 14 μL of reagent diluent containing bovine serum and 986 μL of PBST. UV curable resin was provided from Toyo Gosei. All other chemicals were obtained from Sigma Aldrich.

Sensor chip fabrication

A plasmonic chip was fabricated by using the UV nanoimprint method followed by depositions of metal and oxide thin films by RF sputtering as described in our previous paper.[20] Briefly, a one-dimensional diffraction grating was created on the microscope slides by the UV nanoimprint method. The silver layer was deposited on the diffraction grating, then thin ZnO and SiO_2 layers were deposited in order to prevent the oxidation of the silver film, and the quenching of the fluorescence emission by a metal. Thin Ti layers were used as an adhesion promotor in between silver/resin and silver/oxide interfaces. The thickness of the silver layer was found to be 37 ± 2 nm by UV-Vis absorption spectroscopy. The thickness of silver was optimized for the excitation of SPs by the rear coupling method and the enhancement of the electromagnetic field.[21] PDA coating was performed by following the procedure

reported previously.[22] 2 mg mL^{-1} dopamine solution in Tris buffer (10 mM, pH 8.5) was applied to the sensor surface, and incubated for 20 min, followed by rinsing with MilliQ water and drying with a nitrogen stream. The thickness of the PDA films can be tuned by the incubation time of the dopamine solution. Under these conditions, the thickness of the PDA film was estimated to be 2 to 3 nm which was considered to be optimal for the SPF measurement.[23] The PDA coated sensor chips were kept in a vacuum desiccator until the immobilization process of the capture antibody was performed.

Detection assay

A sandwich immunoassay was employed for the detection of NSE with biotinylated detection antibody (d-Ab) and Cy5 labelled streptavidin (Cy5-SA) utilizing the biotin–avidin system, as depicted in Fig. 1. The immobilization of the capture antibody, NSE, and detection antibody was performed on a shaker before mounting the sensor chip onto the optical setup. In this process, a handmade PDMS cuvette consisting of a PDMS sheet with a punched hole with a diameter of 8 mm was attached to the plasmonic chip. The volume of the solution was adjusted to be 40 to 50 μL. The plasmonic chip incorporated with the PDMS cuvette was placed on the shaker, and covered with a Petri dish in order to avoid contamination and evaporation of the solution. After each step, the solution was gently removed and the sensor surface was rinsed three times by using PBS for c-Ab and PBST for all the other steps. For the immobilization of the c-Ab, an anti-NSE capture antibody (c-Ab) solution adjusted to be 75 μg mL^{-1} in PBS was applied to the sensor surface, and the substrate was shaken for 15 min. After the rinsing process, the assay diluent containing bovine serum was introduced to the sensor surface and shaken for 5 min as a blocking agent in order to suppress the non-specific binding of NSE and the detection antibody. The samples containing NSE were prepared in the assay diluent or diluted human serum in various concentrations from 0.125 ng mL^{-1} up to 125 ng mL^{-1}. The sample solution containing NSE was brought in contact with the sensor surfaces and shaken for 15 min. The biotinylated detection antibody adjusted to be 2.5 μg mL^{-1} in the assay diluent was applied to the sensor surface and shaken for 10 min. The sensor chip was then mounted to the optical setup, and 10 nM Cy5-SA solution was introduced to the sensor surfaces for 5 min followed by rinsing with PBST. Angular resolved reflectivity and fluorescence intensity spectra were taken before and after injection of Cy5-SA solution. The total assay time including the immobilization of the capture antibody was within 60 min. The experiments of the immunoassay were repeated at least three times by using different plasmonic chips fabricated by the same protocol, and the standard deviations of the experimental results were obtained which are described as the error bars.

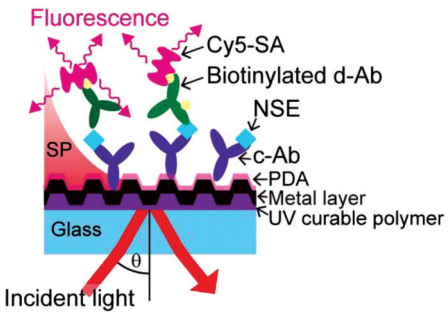

Fig. 1 Schematic drawing of the plasmonic chip and the detection assay.

Optical setup

A home-build optical setup with a two-axis motorized rotation stage was used for the angular reflectivity and fluorescence intensity measurement, as shown in Fig. S1 in the ESI.† The beam from the He–Ne laser (λ = 632.8 nm, 05-LHP-151, Melles Griot) passed the chopper and polarizers before incident light to the sensor chip from the rear panel formed. A set of polarizers were used to adjust the laser beam intensity and to make the incident light p-polarized. The two-axis motorized rotation stage (SGSP-120YAW-W, Sigma Koki) was used to control the angle of incident θ and the detection angle at 2θ. The intensity of the reflected laser beam was detected by using the chopper and a photodiode with a lock-in amplifier (7265, PerkinElmer). The fluorescence signals emitting into the direction of the aqueous solution were collected by using a set of lenses (AC254-040-A-ML and AC245-06-A, Thorlabs) and filters (FL670-10, Tholabs, and BLP01-635R-25, Semrock). The fluorescence intensity was detected by using a photomultiplier tube with the counter (53131A, Agilent). A PDMS cuvette (volume of 80 μL) was attached to the sensor surface in order to allow the flow of the aqueous solution. The aqueous solution including the samples and buffer was introduced by using an injection syringe. The optical setup was controlled by using the software Wasplas developed at the Max Planck Institute for Polymer Research (MPIP) in Mainz, Germany.

Results and discussion

Characterization of the plasmonic chip

A representative photograph of the fabricated plasmonic chip is shown in Fig. 2a. The grating structure was created in the area of 4 × 4 mm^2 as projected in a bluish color in the center of the substrate as the result of iridescence. The grating structure is observed by Atomic Force microscopy (AFM) as shown in Fig. 2b. The uniform periodic structure of one-dimensional grating consisting of lines and spaces was observed, confirming the successful replication of the grating structure. The averaged pitch and the modulation depth of the grating were 491 ± 10 nm and 32 ± 2 nm, respectively. The duty ratio defined as the ratio of the convex part and the pitch was 0.45. The surface roughness of the grating structure (R_a) was 1.6 nm. For the excitation of the GC-SPR, the grating structures including the pitch and the depth of the modulation as well as the metal thickness are crucial parameters which decide the resonance

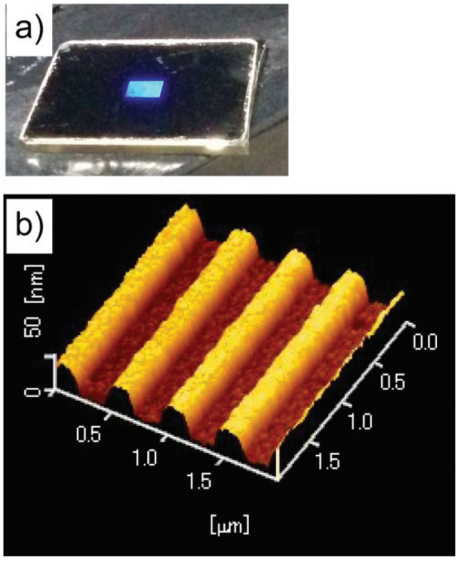

Fig. 2 (a) A representative photograph and (b) an AFM image of the fabricated plasmonic chip.

conditions and field enhancement factors. The structure of the plasmonic chip fabricated in this study was optimized for the excitation of SP at a wavelength of around 630 nm by using the rear-side coupling scheme.[21,24,25]

Before performing the immunoassay, the amount of immobilized capture antibody was estimated by using SPR spectroscopy. In this experiment, the prism coupling scheme was employed for the quantitative analysis utilizing the Fresnel equations. Let us note that it is complicated to analyze the SPR curve obtained from the GC-SPR method. The plasmonic chip was attached to the prism by rotating 90 deg in order to avoid diffraction based excitation of SPR. The angular reflectivity spectra were obtained in water before and after immobilization of c-AB in both inside and outside grating structures. By fitting the SPR curves as described elsewhere,[19] the surface mass densities of the attached c-Ab were estimated to be 2.5 ± 0.2 and 2.1 ± 0.2 ng mm^{-2} inside and outside the grating structure, respectively. The slightly larger amount of c-Ab was attached to the grating structure likely due to the increased surface areas. The surface mass density of the attached c-Ab on the plasmonic chip was comparable to the value obtained with the planar gold substrate coated with PDA which was fully covered with similar IgG molecules.[19] Therefore, we considered that the surface of the plasmonic chip was mostly covered with the c-Ab.

Detection of NSE by SPF spectroscopy

Firstly, NSE dissolved in the assay diluent at a high concentration was measured. In this experiment, the concentration of NSE was adjusted to 125 ng mL^{-1} in the assay diluent. The angular resolved reflectivity and fluorescence intensity spectra were recorded before and after the introduction of the Cy5 labelled streptavidin (Cy5-SA), see Fig. 3a and b. As shown in Fig. 3a, there is a reflectivity drop around 22 deg associating

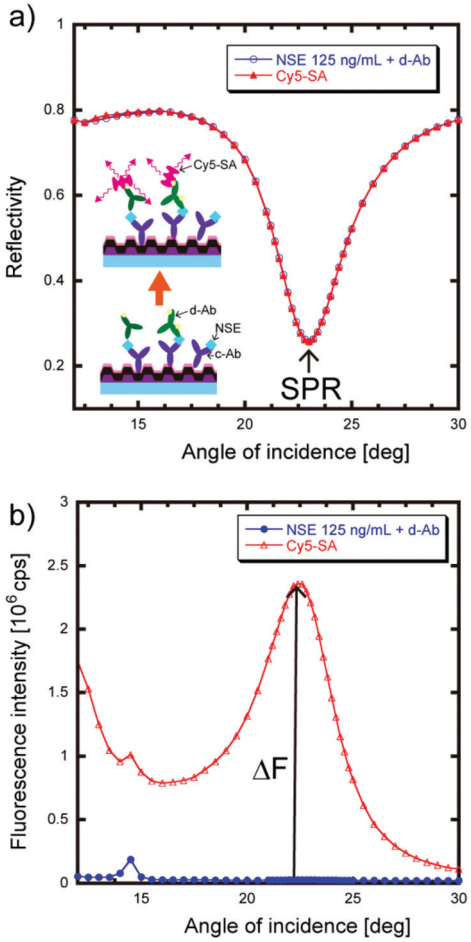

Fig. 3 Angular resolved (a) reflectivity and (b) fluorescence intensity spectra taken before (blue) and after the injection of the Cy5-SA (red).

the excitation of grating coupled surface plasmon resonance (GC-SPR), which is in good agreement with the previous study performed with a similar grating structure and the optical setup.[21] Let us note that the resonance angles of GC-SPR highly depend on the grating pitch as well as the composition of the layer structure, *e.g.* metal species, surrounding media, and the wavelength of the incident light.[26] The adsorption of Cy5-SA did not cause the measurable shift in the resonance angle in Fig. 3a. In contrast to the reflectivity spectra, the fluorescence intensity dramatically increased around the resonance angle after the injection of Cy5-SA followed by rinsing with PBST indicating that the employed detection assay worked properly. The appearance of the peak in the fluorescence intensity around the resonance angle is attributed to the enhanced electro-magnetic field of SPs in the vicinity of the sensor surface.

Calibration curve for the detection of NSE in buffer solution

The calibration curve for the detection of NSE dissolved in buffer solution was obtained. The samples containing NSE at various concentrations from 0 ng mL^{-1} to 125 ng mL^{-1} were detected. The error bars associating with the variation of the sensor response among the different sensor chips were

obtained by repeating the experiment more than three times with different sensor chips and described as the standard deviation. The angular resolved reflectivity and fluorescence intensity spectra were obtained before and after injection of Cy5-SA followed by rinsing with PBST. The fluorescence signal ΔF was obtained by subtracting the background signal from the fluorescence intensity at the incident angle where the fluorescence intensity reached its maximum, as depicted in Fig. 3b. The blank sample (0 ng mL^{-1}) was measured for the evaluation of the signals caused by the non-specific binding of d-Ab and Cy5-SA with the same assay procedure. Fig. 4 shows the plot of fluorescence signal ΔF as a function of NSE concentration. The fluorescence signals increased as the concentration of NSE increased, and an approximately linear sensor response was obtained at the concentration range from 1 ng mL^{-1} to 100 ng mL^{-1}. For the lower concentration (NSE concentration <0.375 ng mL^{-1}), the fluorescence signal is converged to certain value induced by the non-specific binding (*ca.* 7100 cps). Let us note that the fluorescence signals induced by the non-specific binding were suppressed by using the blocking agent roughly by a factor of three. Nevertheless, non-specific adsorption of the detection antibody and Cy5-SA onto the sensor surface still existed to some extent. These non-specific bindings with the sensor surfaces after treatment with the blocking agent were also reported by other studies achieving the sensitive detection of the target analytes.[6,10,29] The experimental data were fitted with the modified Langmuir-isotherm in order to estimate the affinity constant described as follows,[6]

$$\Delta F = F_u \cdot K_a \cdot c_{NSE} / (1 + K_a \cdot c_{NSE}) + F_n$$

where F_u denotes the upper asymptotic value of fluorescence signals, K_a denotes the apparent affinity constant of the detection antibody against NSE, c_{NSE} is the concentration of NSE and F_n denotes the fluorescence signals by non-specific adsorption. The fitted curve is plotted as a solid line in Fig. 4. For fitting, an approximated upper asymptotic value F_u was used, which resulted in a high coefficient of determination (R^2 = 0.998). From the fitting result, the apparent affinity constant K_a was estimated to be 6.3 × 10^5 g^{-1} mL, corresponding to the dissociation constant of K_d = 3.5 × 10^{-8} M. The obtained dissociation constant for this experiment is in the same range of general K_d (10^{-8} to 10^{-10} M). A linear approximation was employed for the low concentration region as there is a slight deviation between the experimental data and the Langmuir-isotherm curve. The experimental results for the low concentration region were plotted in the linear scale and the linear approximation was determined. The limit of detection (LOD) for NSE in the buffer solution was determined as the intersection between the fitted curve and the value of the F_n plus three times of the standard deviation 3σ indicated in the inset in Fig. 4. The obtained LOD is 0.5 ng mL^{-1} (11 pM) for NSE in the assay diluent which is sufficiently below the clinical relevant value at 12–13 ng mL^{-1}.

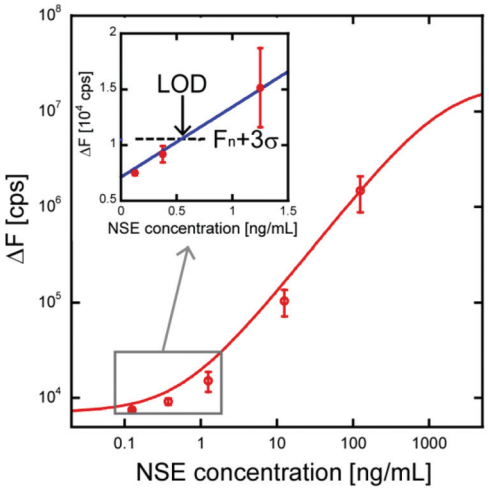

Fig. 4 Calibration curve for the detection of NSE in a buffer solution plotting the fluorescence signals as a function of the NSE concentration. The inset is the linear approximation for the low concentration region. The limit of detection (LOD) is indicated where the fitted curve meets the cut-off value determined by the fluorescence signals associated with the non-specific binding (F_n) and the three times of its standard deviation (3σ).

Calibration curve for the detection of NSE in human serum

Furthermore, the sensing performance of the developed SPF biosensor was investigated for the detection of NSE dissolved in human serum. Before demonstrating the detection of NSE, we characterized the sensing performance in terms of the fluorescence signal induced by the non-specific binding for the blank sample (NSE: 0 ng mL^{-1}). The solutions containing human serum diluted to PBST at various dilution ratios (0, 25, 50 and 100 vol%) were measured as blank samples in the assay procedure. As shown in Fig. S2 in the ESI,† the fluorescence signal increased as the concentration of human serum increased. It indicates that the non-specific adsorption of the serum components, and detection antibody and/or Cy5-SA increased as the concentration of human serum raised. Accompanied by the increment of the F_n, the error bars obtained enhanced indicating that the reproducibility is decreased for the measurement of the sample dissolved in human serum. The fluorescence signal due to the non-specific binding is suppressed by diluting the human serum with the PBST buffer. For further experiment, we employed 25 vol% human serum in PBST for the detection of NSE. By using a diluted solution, the required sample volume can be reduced to 10 μL, as 40 μL solution after dilution is sufficient for the measurement in our system.

The NSE sample dissolved in the diluted human serum (25 vol%) was prepared in the same concentration range as the previous experiment and fluorescence signals were detected. The plot of the fluorescence signal against the NSE concentration in the diluted human serum is shown in Fig. 5. In Fig. 5, the larger non-specific binding and the error bars were obtained with respect to that obtained with the NSE in the buffer solution. Nevertheless, the linear sensor response in the concentration range from 1 ng mL^{-1} to 100 ng mL^{-1} was obtained, indicating that the developed NSE biosensor works

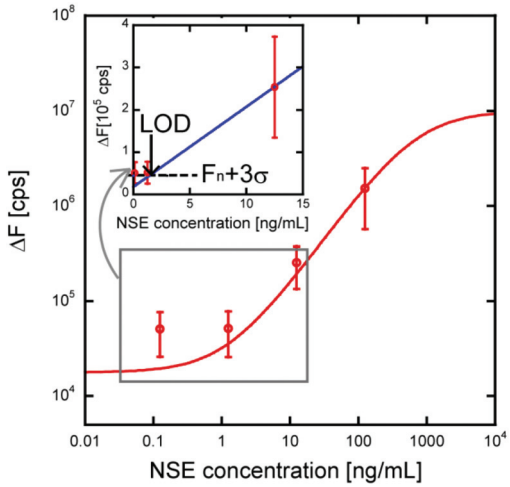

Fig. 5 Calibration curve for the detection of NSE dissolved in the diluted human serum. The inset is the linear approximation for the low concentration region.

properly for the detection of the sample in serum. By fitting the experimental data with the modified Langmuir-isotherm, a fitting curve shown in Fig. 5 as a solid curve is determined. The fitting was performed in the same manner as Fig. 5, and resulted in a high coefficient of determination of R^2 = 0.998. The apparent affinity constant K_a was calculated to be 2.2×10^6 g^{-1} mL, which can be translated to 9.8×10^{-9} M in dissociation constant K_d. The estimated K_d value is slightly lower than that obtained for the sample in the buffer solution, nevertheless still in the same concentration range, indicating that the affinity interactions between the NSE and antibodies were retained even in the human serum containing a large amount of various proteins. Let us note that the affinity interactions between the antigen and antibody can be influenced by the solution, as the former study has reported the inhibited affinity interaction in the complex solution such as human serum resulting in the increased K_d values.[27] The LOD for NSE was determined by the same manner as the previous experiments by using the linear approximation as shown in the inset of Fig. 5, and to be 1.4 ng mL^{-1} (30 pM). This value corresponds to the serum concentration of 5.6 ng mL^{-1}. The obtained LOD is about one order of magnitude worse than that obtained with the buffer solution, but still it is below the clinical relevant value even considering that the sample is diluted with the buffer solution. We attribute the degraded detection LOD to the enhanced non-specific binding in human serum as reported in the other publications.[5,28]

The sensitive detection of NSE has been performed by using the various detection schemes as summarized in Table 1. The comparable LOD for the detection of NSE has been reported by using the plasmon enhanced fluorescence (PEF) on the gold island arrays with a micro-array format enabling a parallel detection of multiple analytes performed with a longer incubation time of NSE (2 hours).[10] A field effect transistor (FET)-based biosensor has been reported to be able

Table 1 Summary of the detection sensitivity of NSE obtained by different detection schemes

Method	LOD [ng mL^{-1}]	Medium	Incubation time of NSE	Ref.
SPFS (this study)	0.5/1.4	Buffer/diluted human serum	15 min	—
PEF	0.15	Pure water	2 hours	10
FET	10/100	Buffer/human serum	n/a	28
Magnetic nanobeads-based LFIA	0.1	Buffer	n/a	30

to detect NSE down to 10 ng mL^{-1} and 100 ng mL^{-1} in a buffer solution and in serum, without using the detection antibody.[29] The highly sensitive detection of NSE at concentration levels of pg mL^{-1} was achieved by using a photoelectrochemical immunosensor utilizing specially synthesized quantum dots.[30] A lateral flow immunoassay (LFIA) employing magnetic nanobeads has been developed for the detection of NSE in the concentration range of 1 to 100 ng mL^{-1}, and the detection limit of NSE was determined to be 0.1 ng mL^{-1}.[31] Our SPF biosensor for the detection of NSE can provide the sufficiently high detection sensitivity below the clinical cut-off value. The rapid detection of NSE was performed by a short incubation time of the sample containing NSE (15 min), and the simplified procedure completed within 60 min including the immobilization process of c-Ab. The presented biosensor scheme requires a small amount of the sample down to 10 μL, which holds the potential for less-invasive analysis of NSE in the serum sample. Furthermore, the combination of a plasmonic chip and the PDA coating technique can be applied for the fabrication of the protein microarray and parallel detection of the multiple analyte by a microscopic measurement with a controlled excitation of SPs.

Conclusions

In this study, rapid and sensitive detection of a tumor marker, neuron specific enolase, was performed by using a plasmonic chip functionalized by a bioinspired polydopamine (PDA) coating. The PDA coating was applied to the disposable silver plasmonic chip as an easy, quick and cheap surface modification technique for the immobilization of the capture antibody onto the sensor surface. A plasmonic chip consisting of a metal coated diffraction grating was employed for the amplification of fluorescence signals in the fluorescence sandwich immunoassay by the enhanced electromagnetic field of propagating surface plasmons. The rear coupling scheme was introduced for the excitation of GC-SPR. The sensing performance in terms of detection sensitivity of NSE and fluorescence signals induced by the non-specific binding were characterized for the sample in the assay diluent and in human serum. The approximately linear sensor responses were obtained for the concentration of NSE from 1 to 100 ng mL^{-1} both in a buffer solution and in a diluted human serum, which covers the clini-

cal cut-off value (16–25 ng mL^{-1}). The determined limit of detection for NSE was 0.5 ng mL^{-1} (11 pM) and 1.4 ng mL^{-1} (30 pM) for the sample in the buffer and in the diluted human serum, respectively, corresponding to 5.6 ng mL^{-1} in the serum. Through the experimental results, the usability of PDA coating for the surface modification of the silver plasmonic chip, and for the detection of biomolecules dissolved in human serum was confirmed. Furthermore, we achieved the sensitive detection of NSE with the small amount of the sample (10 μL in human serum) and a short assay time within 60 min by using the presented biosensor scheme. This is the first example of the usage of a plasmonic chip functionalized with a PDA coating combined with the rear-coupling scheme for the sensitive detection of biomarkers in a complex solution, namely human serum. The presented SPF biosensor scheme based on the PDA coated plasmonic chip may be a promising tool for the detection of target analyte in a clinical sample by a simple and less-invasive manner.

Conflicts of interest

There are no conflicts to declare.

Acknowledgements

This work was supported by JSPS KAKENHI Grant Numbers, JP15H06766 in Research Activity Start-up, JP16H02092 in Scientific Research (A) and MEXT KAKENHI Grant Number JP15H0110 in Scientific Research on Innovative Areas "Photosynergetics".

MT, SI and KT thank Toyo Gosei Co. for providing the UV-curable resin.

Notes and references

1 Z. Altintas and I. Tothill, *Sens. Actuators, B*, 2013, **188**, 988–998.
2 S. A. Soper, K. Brown, A. Ellington, B. Frazier, G. Garcia-Manero, V. Gau, S. I. Gutman, D. F. Hayes, B. Korte, J. L. Landers, D. Larson, F. Ligler, A. Majumdar, M. Mascini, D. Nolte, Z. Rosenzweig, J. Wang and D. Wilson, *Biosens. Bioelectron.*, 2006, **21**, 1932–1942.
3 M. Bauch, K. Toma, M. Toma, Q. Zhang and J. Dostalek, *Plasmonics*, 2014, **9**, 781–799.
4 S. H. Cao, W. P. Cai, Q. Liu and Y. Q. Li, *Annu. Rev. Anal. Chem.*, 2012, **5**, 317–336.
5 Y. Wang, A. Brunsen, U. Jonas, J. Dostalek and W. Knoll, *Anal. Chem.*, 2009, **81**, 9625–9632.
6 K. Tawa, F. Kondo, C. Sasakawa, K. Nagae, Y. Nakamura, A. Nozaki and T. Kaya, *Anal. Chem.*, 2015, **87**, 3871–3876.
7 K. Tawa, H. Hori, K. Kintaka, K. Kiyosue, Y. Tatsu and J. Nishii, *Opt. Express*, 2008, **16**, 9781–9790.
8 K. Tawa, M. Satoh, K. Uegaki, T. Hara, M. Kojima, H. Kumanogoh, H. Aota, Y. Yokota, T. Nakaoki and M. Umetsu, *Jpn. J. Appl. Phys.*, 2013, **52**, 06GK01.
9 K. Aslan, J. Huang, G. M. Wilson and C. D. Geddes, *J. Am. Chem. Soc.*, 2006, **128**, 4206–4207.
10 B. Liu, Y. L. Li, H. Wan, L. Wang, W. Xu, S. J. Zhu, Y. Liang, B. Zhang, J. Lou, H. Dai and K. Qian, *Adv. Funct. Mater.*, 2016, **26**, 7994–8002.
11 K. Tawa, M. Umetsu, H. Nakazawa, T. Hattori and I. Kumagai, *ACS Appl. Mater. Interfaces*, 2013, **5**, 8628–8632.
12 O. C. Burghuber, B. Worofka, G. Schernthaner, N. Vetter, M. Neumann, R. Dudczak and R. Kuzmits, *Cancer*, 1990, **65**, 1386–1390.
13 A. Jemal, R. Siegel, E. Ward, Y. P. Hao, J. Q. Xu, T. Murray and M. J. Thun, *CA-Cancer J. Clin.*, 2008, **58**, 71–96.
14 T. Esscher, L. Steinholtz, J. Bergh, E. Nöu, K. Nilsson and S. Påhlman, *Thorax*, 1985, **40**, 85–90.
15 F. Barlesi, C. Gimenez, J. P. Torre, C. Doddoli, J. Mancini, L. Greillier, F. Rouxe and J. Kleisbauer, *Respir. Med.*, 2004, **98**, 357–362.
16 H. Lee, S. M. Dellatore, W. M. Miller and P. B. Messersmith, *Science*, 2007, **318**, 426–430.
17 R. A. Zangmeister, T. A. Morris and M. J. Tarlov, *Langmuir*, 2013, **29**, 8619–8628.
18 M. E. Lynge, R. van der Westen, A. Postma and B. Stadler, *Nanoscale*, 2011, **3**, 4916–4928.
19 M. Toma and K. Tawa, *ACS Appl. Mater. Interfaces*, 2016, **8**, 22032–22038.
20 N. Akashi, K. Tawa, Y. Tatsu, K. Kintaka and J. Nishii, *Jpn. J. Appl. Phys.*, 2009, **48**, 06FH17.
21 K. Tawa, Y. Yokota, K. Kintaka, J. Nishii and T. Nakaoki, *Sens. Actuators, B*, 2011, **157**, 703–709.
22 J. B. Wood, M. W. Szyndler, A. R. Halpern, K. Cho and R. M. Corn, *Langmuir*, 2013, **29**, 10868–10873.
23 M. Toma and K. Tawa, *Jpn. J. Appl. Phys.*, DOI: 10.7567/JJAP.57.03EK01.
24 X. Q. Cui, K. Tawa, H. Hori and J. Nishii, *Adv. Funct. Mater.*, 2010, **20**, 546–553.
25 H. Hori, K. Tawa, K. Kintaka, J. Nishii and Y. Tatsu, *J. Appl. Phys.*, 2010, **107**, 114702.
26 W. Knoll, *Annu. Rev. Phys. Chem.*, 1998, **49**, 569–638.
27 C. J. Wienken, P. Baaske, U. Rothbauer, D. Braun and S. Duhr, *Nat. Commun.*, 2010, **1**, 1–7.
28 B. B. Haab, M. J. Dunham and P. O. Brown, *Genome Biol.*, 2001, **2**, 0004.
29 S. Cheng, S. Hideshima, S. Kuroiwa, T. Nakanishi and T. Osaka, *Sens. Actuators, B*, 2015, **212**, 329–334.
30 X. Y. Yu, Y. Y. Wang, X. M. Chen, K. B. Wu, D. C. Chen, M. Ma, Z. Huang, W. Wu and C. Li, *Anal. Chem.*, 2015, **87**, 4237–4244.
31 W. Lu, K. Wang, K. Xiao, W. Qin, Y. Hou, H. Xu, X. Yan, Y. Chen, D. Cui and J. He, *Sci. Rep.*, 2017, **7**, 42414.